J. Fac. Edu. Saga Univ.
Vol.18, No. 2(2014) 49～63

The NQR and X-ray Study of Mercuric Chloride Complexes

Asuka KOGA, Emiko YAMAKAWA, Michio NAKASHIMA, Hideta ISHIHARA

Summary

^{35}Cl NQR spectra of Hg_3OCl_4, Cs_3HgCl_5, Cs_2HgCl_4, $CsHgCl_3$, $CsHg_2Cl_5$, and $CsHg_5Cl_{11}$were observed and their temperature dependences of NQR frequencies were measured. The structures of these complexes are discussed on the basis of the results of NQR measurements and powder X-ray diffraction.

Key words: ^{35}Cl NQR, Powder X-ray pattern, Mercuric chloride complex

Introduction

The existence of mercuric halide complex salts is widely known in the various systems including mercuric chloride ($HgCl_2$). In certain complex salts, the ferroelectric property (*e.g.* $(CH_3)_4NHgI_3$) and pyroelectric property (*e.g.* Cs_2HgI_4) have been found. We try to confirm the existence of $HgCl_2$ complex salts and investigate structures by means of Nuclear Quadrupole Resonance (NQR) and X-ray diffraction measurements.

Results and Discussion

The system of $HgCl_2 - NaOH - H_2O$

Weiss *et al.* reported that $Hg_3OCl_4(2HgCl_2{\cdot}HgO)$ and $Hg_3O_2Cl_2(HgCl_2{\cdot}2HgO)$ were formed in the ternary system of $HgCl_2$–$NaOH$–H_2O at 20℃ [1]: After mixing suitable proportion of components, colloidal $Hg_3O_2Cl_2$ precipitated and this precipitate turned out to be colorless cubic crystal Hg_3OCl_4 in about ten months. We tried to prepare $Hg_3O_2Cl_2$ according to Ref. [2], but we could not get enough amount of crystalline $Hg_3O_2Cl_2$ to observe NQR. We prepared Hg_3OCl_4 and executed ^{35}Cl NQR measurement and X-ray diffraction. The ob-

Table1. The observed ^{35}Cl NQR frequencies of Hg_3OCl_4.

T (K)	77	273
ν (MHz)	22. 30	21. 91

$HgCl_2$ shows two ^{35}Cl NQR lines of 22.87 and 22.52 MHz at 77 K, and 22.26 and 22.07 MHz at 294 K.

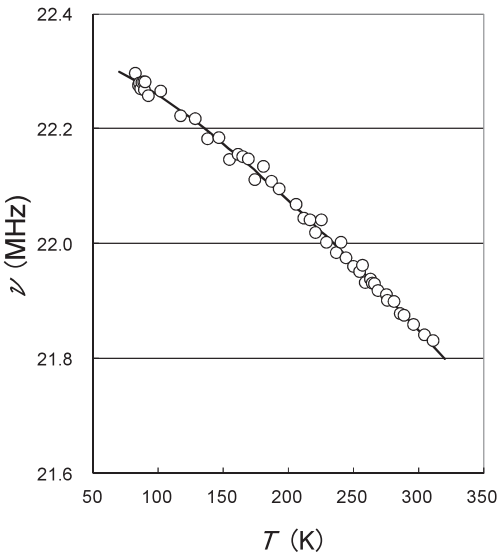

Fig. 1. The temperature dependence of ^{35}Cl NQR frequencies of Hg_3OCl_4. The solid line shows the fitting curve by least-squares method (Appendix I).

Faculty of Culture and Education, Saga University, Honjo-machi 1, Saga 840-8502, Japan
Reprint requests to Prof. H. I. E-mail: isiharah@cc.saga-u.ac.jp

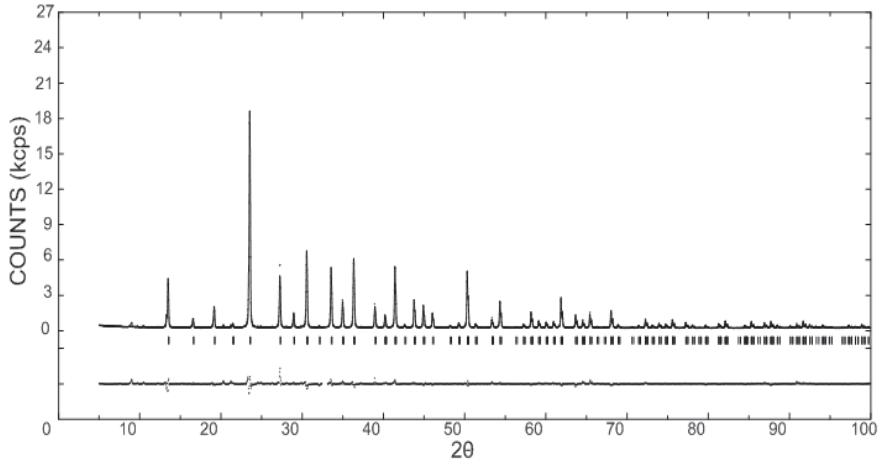

Fig. 2. The powder X-ray pattern at room temperature. Upper curve: the calculated pattern by Rietveld analysis (solid line) and observed pattern (broken line). Lower curve: the difference between observed pattern and the calculated pattern, the bar shows the position of calculated diffraction peak.

served ^{35}Cl NQR frequencies of Hg_3OCl_4 at representative temperatures are listed in Table 1. The temperature dependence of NQR frequencies is depicted in Fig. 1 and coefficients of temperature dependence following the equation of $\nu = a + b/T + c \times T + d \times T^2$ by means of the least-squares method using PC application software EXCEL are listed in Appendix I. One ^{35}Cl NQR line was observed at each temperature between 77 and 310 K. This fact is in agreement with the report by Weiss *et al.* [1] which indicates that there is one kind of chlorine atom in the crystal.

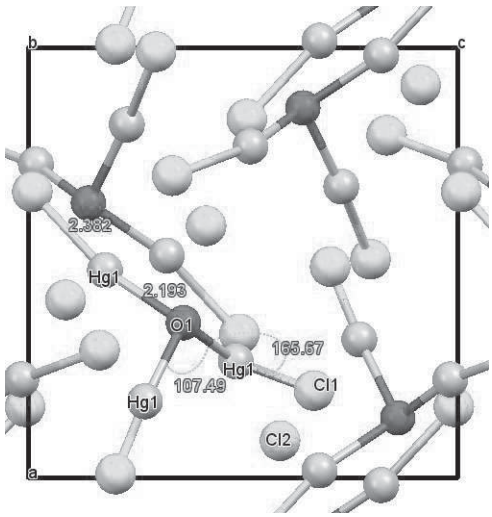

Fig. 3. The view of crystal structure of Hg_3OCl_4 on *bc* −plane along *a*−axis from MERCURY 3.1.1 [3].

We tried to carry out Rietveld analysis of powder X-ray pattern by use of RIETAN 2000 [3].

The result of Rietveld analysis is shown in Fig. 2 and indicates that Hg_3OCl_4 is cubic; the space group is $P2_13$, with a= 9.2341(2) Å and Z = 4 (See atomic coordinates in Appendix II). The evaluation parameters are R_{wp}=8.96, R_p=6.36, R_e=4.59, and S=1.95. This result is in accord with the report by Weiss *et al.* that the space group is $P2_13$ with a=9.26(1) Å [1]. Fig. 3 shows the view of the crystal structure along *a*−aixs.

The determined structure is slightly different from the result by Weiss *et al.* They indicated the existence of $O(HgCl)_3^+$ ion with O−Hg=2.06 Å, Hg −Cl_1=2.40 Å, Hg−Cl_2=2.95 Å, ∠Hg−O−Hg'=120.0° and Cl_1−Hg−O=179.85°. On the other hand, our result shows that $O(HgCl)_3^+$ ion has the conformation with ∠Hg−O−Hg'=107.49°, ∠Cl_1−Hg−O=165.6°, O−Hg=2.193 Å and Hg−Cl_1=2.382 Å with the shortest contact of Hg−Cl_2=2.926 Å. One observed ^{35}Cl NQR line must be attributed to the Cl_1 atom taking the shortest Hg−Cl bond length into consideration. This bond length is slightly longer

than Hg−Cl=2.23 and 2.27 Å in $HgCl_2$ which gives two NQR lines in the range of 22 MHz. The Cl_1 atom of Hg_3OCl_4 gives the slightly lower frequency than those of $HgCl_2$, being in accordance with the dependence of ^{35}Cl NQR frequency on the Hg−Cl bond length such as $\nu \propto 1/d(\mathrm{Hg-Cl})^3$. The Cl_2 atom is surrounded by six Hg atoms at distances of 2.926 Å ×3 and 3.098 Å ×3. Therefore, the NQR line assigned to the Cl_2 atom may be observed lower than 8.5 MHz, below the limit of our instrument.

The system of $HgCl_2$−CsCl

Foote *et al.* reported that the stable double salts were Cs_3HgCl_5, Cs_2HgCl_4, $CsHgCl_3$, $CsHg_2Cl_5$, and $CsHg_5Cl_{11}$ in the ternary system of CsCl−$HgCl_2$−H_2O at 25°C [4]. On the other hand, Kirilenko *et al.* reported that all sorts of double salts mentioned were stable compounds in the system of CsCl−$HgCl_2$ from the results of measurement of differential thermal analysis (DTA) and NQR [5]. Most of all Cs_2HgCl_4 is very intriguing and has been studied intensively using various methods including NQR, because it shows the sequence of incommensurate and commensurate superstructures while varying temperature [S1] and the other double salts are also interesting because of possibility of ferroelectric compounds.

Cs_3HgCl_5

Clegg *et al.* reported that Cs_3HgCl_5 is orthorhombic, *Pnma*, a=8.916(1), b=10.772(1), c=13.505(1) Å, Z=4 [6]. We tried to execute Rietveld analysis on the basis of space group *Pnma*, the result was not so good: the evaluation parameters are R_{wp}=22.08, R_p=14.42, R_e=5.59, and S=3.95. Taking the eutectic system of Cs_3HgCl_5−Cs_2HgCl_4 [5] into consideration, we tried the two-phase analysis and calculated patterns are shown in Fig. 4. The evaluation parameters were a little improved: R_{wp}=18.93, R_p=13.34, R_e=5.58 and S=3.29 with Cs_3HgCl_5 (estimate of content by percentage: 85%)

Table 2. The observed ^{35}Cl NQR frequencies of Cs_3HgCl_5.

T (K)	85	273
ν (MHz)	13. 51, 14. 25	13. 29, 13. 81

13.16 MHz at 77 K [5].

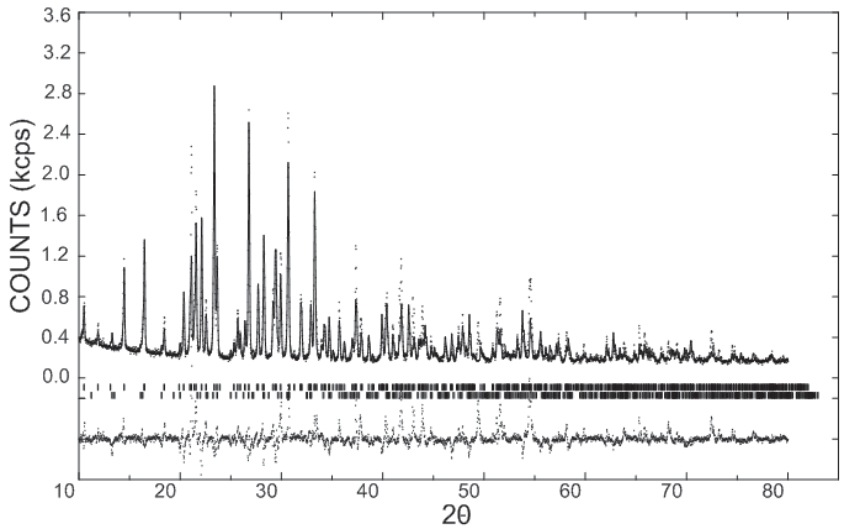

Fig. 4. The powder X-ray pattern of Cs_3HgCl_5+Cs_2HgCl_4 at room temperature. Upper curve: the calculated pattern by Rietveld analysis (solid line) and the observed pattern (broken line). Lower curve: the difference between observed pattern and the calculated pattern, the bar shows the position of calculated diffraction peak.

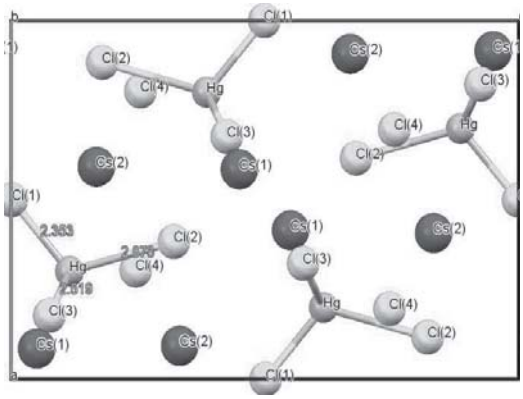

Fig. 5. The view of the crystal structure of Cs_3HgCl_5 along *b*-axis on *ac*−plane from MERCURY 3.1.1. The *ac*−plane is the mirror plane.

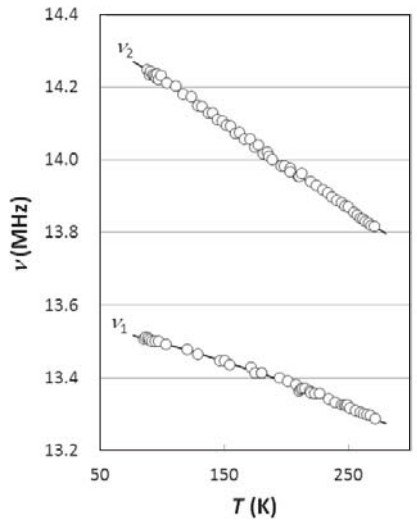

Fig. 6. The temperature dependence of ^{35}Cl NQR Frequencies of Cs_3HgCl_5. The solid line shows the fitting curve by least-squares method (Appendix I).

and Cs_2HgCl_4 (15%) and lattice parameters and atomic coordinate are listed in Appendix II. The crystal of Cs_3HgCl_5 consists of two Cs^+ ions and $HgCl_4^{2-}$ ion with *Cs* symmetry and Hg−Cl_1=2.353, Hg−Cl_2=2.873, and Hg−Cl_3(Cl_3')=2.519 Å as illustrated in Fig. 5, but Clegg *et al.* reported that Hg−Cl_1=2.441, Hg−Cl_2=2.540, and Hg−Cl_3(Cl_3')=2.438 Å [6].

Two ^{35}Cl NQR lines could be observed at room temperature as listed in Table 2. The intensity ratio is 2:1 with decreasing−frequency order.

Table 3. The observed ^{35}Cl NQR frequencies of metastable Cs_4HgCl_6.

T (K)	85	273
ν (MHz)	13. 21	12. 87

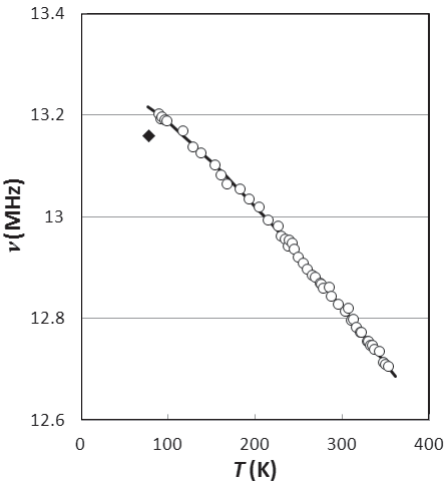

Fig. 7. The temperature dependence of ^{35}Cl NQR frequencies of metastable Cs_4HgCl_6. Solid line shows the fitting curves by the least-squares method (Appendix I). The diamond square shows the result by Kirilenko *et al.* [5].

Therefore the high−frequency line is assigned to Cl_3(Cl_3')atoms and the low−frequency line is to Cl_1 atoms, according to the dependence of NQR frequency on the bond length, although our result shows that Hg−Cl_3 is longer than Hg−Cl_1. The temperature dependence of ^{35}Cl NQR lines is shown in Fig. 6. Two ^{35}Cl NQR lines were observed and there is no indication of a phase transition at temperatures between 85 and 273 K. Kirilenko *et al.* reported that one NQR line of 13.16 MHz was observed at 77 K [5], but it is not in agreement with our results. According to the crystal structure, three ^{35}Cl NQR lines are supposed to be expected and the NQR line due to the Cl_2 atom may be lower than 8.5 MHz, below the limit of our instrument. In addition, we tried to prepare Cs_4HgCl_6 in the same way as other samples and we could observe one ^{35}Cl NQR immediately after preparation as listed in Table 3 and as

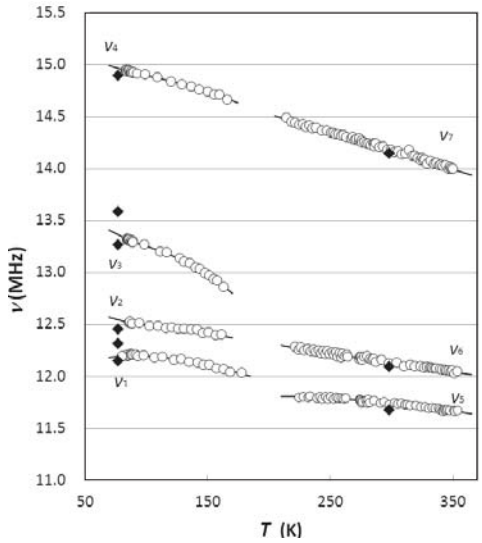

Fig. 8. The temperature dependence of ^{35}Cl NQR frequencies of Cs_2HgCl_4. The solid line shows the fitting curve by least-squares method (Appendix I). The diamond squares show the result by Kirilenko *et al* [5].

Table 4. The observed ^{35}Cl NQR frequencies of Cs_2HgCl_4.

T (K)	85	273
ν (MHz)	12. 20, 12. 52 13. 32, 14. 94	11. 78, 12. 18, 14. 27

10.84, 12.15, 12.32, 12.46, 13.27, 13.59, 14.90, and 16.27 MHz at 77 K. 11.68, 12.10, 14.15 MHz at 293 K [5].

shown in Fig. 7. This ^{35}Cl NQR line observed at liquid nitrogen temperature has almost the same frequency as Cs_3HgCl_5 reported by Kirilenko *et al* [5]. This line could be detected at each temperature between 80 and 350 K as illustrated in Fig. 7, but this NQR line disappeared in several years and then two new NQR lines appeared with the same frequencies of Cs_3HgCl_5 as described above. There is no phase of Cs_4HgCl_6 in the phase diagram reported by Kirilenko *et al.* [5] though, metastable phase of Cs_4HgCl_6 may exist and the disproportionation may occur slowly, and then it turns into CsCl and Cs_3HgCl_5.

Cs_2HgCl_4

The temperature dependence of ^{35}Cl NQR frequencies at temperatures between 80 and around 350 K is shown in Fig. 8. The aspect of temperature dependence is similar to the results reported by Bouslavskii *et al.* [7] except for the low-temperature phase below about 160 K and the intermediate phase between 170 and 180 K. They could observe the eight ^{35}Cl NQR lines in the low-temperature phase, but we could observe only

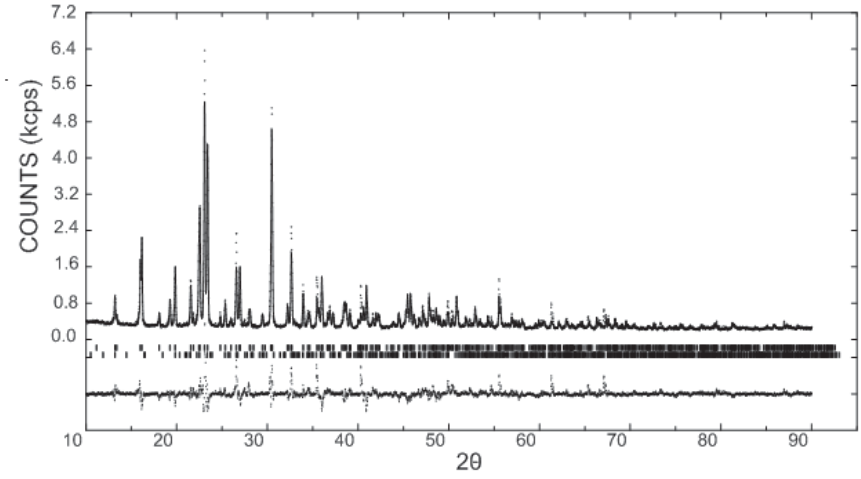

Fig. 9. The powder x-ray pattern of Cs_2HgCl_4+Cs_3HgCl_5at room temperature. Upper curve: the calculated pattern by Rietveld analysis (solid line) and the observed pattern (broken line), Lower curve: the difference between the observed pattern and the simulated pattern, the bar shows the position of calculated diffraction peak.

four ^{35}Cl NQR lines. Three NQR lines appeared at temperatures above about 215 K and this behavior is in the same way as their results. The sample at room temperature was identified by the powder X-ray diffraction method and Rietveld analysis of diffraction pattern. The results by using RIETAN 2000 showed that Cs_2HgCl_4 is orthorhombic, the space group is *Pnma*, with a=9.2804 (5), b=7.6082(4), and c=13.4223(7) Å, and Z=4. The evaluation parameters are R_{wp}=13.58, R_p=9.98, R_e =4.98, and S=2.73. This result is in agreement with the one reported by Linde *et al.* that the space group is *Pnmb* with a=7.585(2), b=9.798(2), and c=13.384(4) Å [8]. On the other hand, Pakhomov *et al.* reported that the crystal was orthorhombic, space group $P2_12_12_1$, with a=7.5994(4), b= 9.8106(9), and c=13.415(2) Å; Z=4 [9]. We tried to simulate the observed X-ray powder pattern on the basis of space group $P2_12_12_1$, but we could not obtain better results than the case of space group *Pnma*. Taking the eutectic system of Cs_3HgCl_5–Cs_2HgCl_4 [5] into consideration, we tried the two-phase analysis: The space group is *Pnma*, with a= 9.8196(5), b=7.6068(4), and c=13.4217(7) Å, and Z=4 (atomic coordinated in Appendix II). The evaluation parameters obtained are a little bit improved: R_{wp}=13.15, R_p=9.76, R_e=4.96 and S=2.65 with Cs_2HgCl_4 (94%) and Cs_3HgCl_5 of space group *Pnma* (6%) (Fig. 9). Also taking the eutectic system of $CsHgCl_3$–Cs_2HgCl_4 [5] into consideration, we tried the two-phase analysis: The space group is *Pnma*, with a=9.8186(5), b=7.6073(4), and c= 13.4223(8) Å, and Z=4. The evaluation parameters obtained are a little improved: R_{wp}=13.67, R_p= 10.10, R_e=4.95 and S=2.76 with Cs_2HgCl_4 (99.9%) and $CsHgCl_3$ of space group $P3_2$ (0.1%). From the results of Cs_3HgCl_5–Cs_2HgCl_4 mixed phase, the

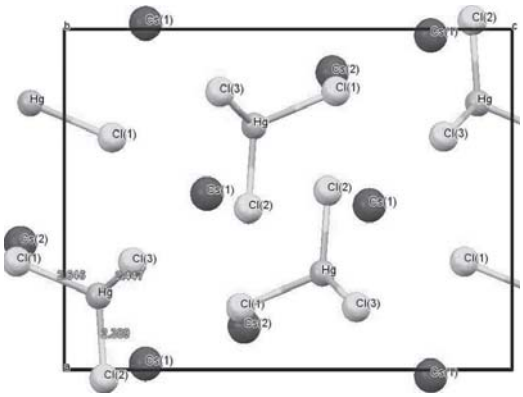

Fig. 10. The view of the crystal structure of Cs_2HgCl_4 along b–axis from MERCURY 3.1.1. The ac–plane is a mirror plane.

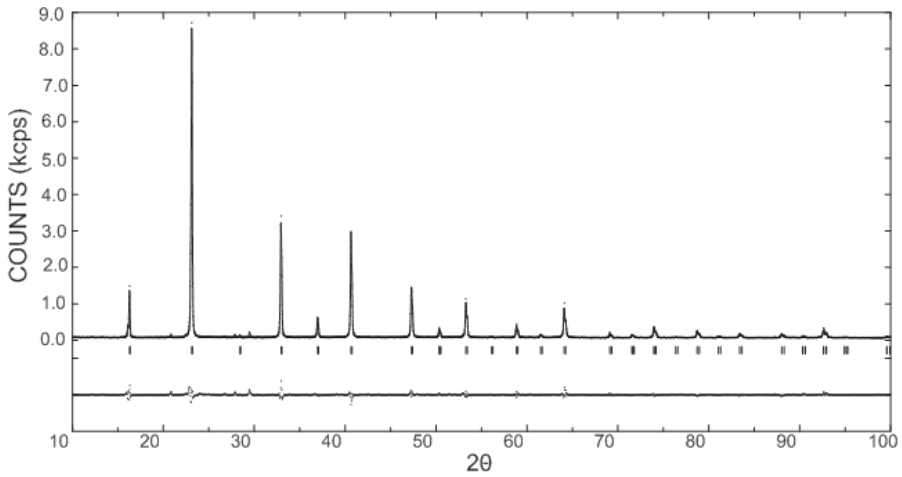

Fig. 11. The powder X-ray pattern of $CsHgCl_3$ at room temperature. Upper curve: the calculated pattern by Rietveld analysis on the basis of space group $Pm3m$ (solid line) and the observed pattern (broken line). Lower curve: the difference between the calculated and the observed patterns.

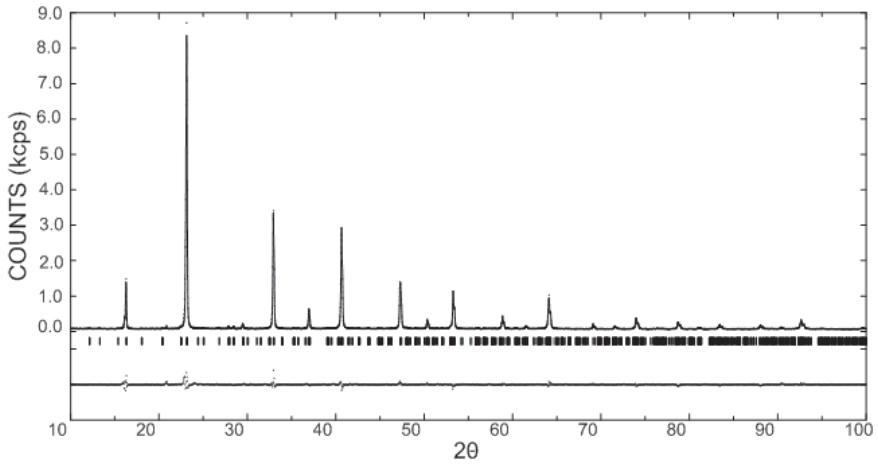

Fig. 12. The powder X-ray pattern of $CsHgCl_3$ at room temperature. Upper curve: the calculated pattern by Rietveld analysis on the basis of space group $P3_2$ (solid line) and the observed pattern (broken line). Lower curve: the difference between the calculated and the observed patterns.

distorted tetrahedral $HgCl_4^{2-}$ ion with *Cs* symmetry exists in this crystal (Fig. 10), of which bond lengths are Hg− Cl_1=2.646, Hg−Cl_2=2.389, and Hg −Cl_3(Cl_3')=2.447 Å. This observation is in agreement with the results of NQR that is three ^{35}Cl NQR lines with intensity ratio of 2:1:1 in decreasing-frequency order at room temperature. The ν_7 NQR line can be assigned to Cl_3 atom in the crystal of Cs_2HgCl_4, and ν_6 and ν_5 to Cl_2 and Cl_1 atoms respectively, judging from the relation of NQR frequency *vs.* bond length, although the bond length of Hg−Cl_2 is the shortest one.

$CsHgCl_3$

This complex salt is reported to be polymorphic at room temperature [10]; cubic form: space group $Pm3m$ with a=5.430 Å, Z=1, orthorhombic from: space group $A2mm$, a=5.429(1), b=7.652(1), c =7.621(1) Å, Z=2. On the other hand, Albarski *et al.* reported $CsHgCl_3$ is trigonal/hexagonal, space group is $P3_2$ with a=13.287(1), c=9.4081(4) Å, and Z =9 [11]. We observed powder X-ray pattern at room temperature and executed Rietveld analysis on the basis of space group $Pm3m$ as shown in Fig. 11: The result of lattice parameters, a=5.4316 (1) Å, Z=1 (atomic coordinates in Appendix II), with the evaluation parameters: R_{wp}=10.70, R_p= 7.70, R_e=8.71, and S=1.23. The simulation of the powder pattern in the case of space group $A2mm$ (standard expression $Cmm2$) was not better than the case of $Pm3m$. Then we tried to simulate the powder X-ray pattern on the basis of space group $P3_2$. By means of Rietveld analysis the fitting curve was obtained as is shown in Fig. 12: This result shows that it is trigonal, space group $P3_2$, a= 13.2976(6), c=9.4177(6) Å, and Z=9 (atomic coordinates in Appendix II) with the evaluation parameters, R_{wp}=10.77, R_p=8.13, R_e=8.63, and S=1.25. The aspect of the calculated pattern in the case of space group $P3_2$ is almost same as the case of $Pm3m$ except for the feature indicated by Albarski *et al.*, that is the small peaks around diffraction angle 2θ ~30° appears in the case of $P3_2$. The result of Rielveld analysis on the basis of space group $Pm3m$ indicates that only one kind of Cl atom exists as asymmetric unit in the crystal. Therefore, one ^{35}Cl NQR line is supposed to be expected, although four ^{35}Cl NQR lines could be observed at

Table 5. The observed ^{35}Cl NQR frequencies of $CsHgCl_3$ (Sample A).

T (K)	88	273
ν (MHz)	18. 65, 18. 90 19. 00, 19. 28	18. 42, 18. 57 18. 70, 18. 95

18.42, 18.57, 18.67, and 18.92 MHz at 293 K [5].

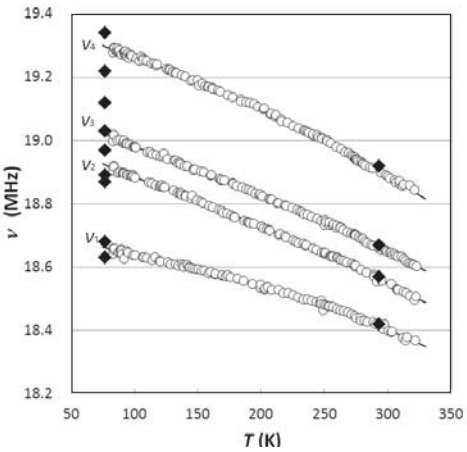

Fig. 13. Temperature dependence of ^{35}Cl NQR frequencies of $CsHgCl_3$ (Sample A). The solid line shows the fitting curve by least-squares method (Appendix I). The diamond shapes show the result by Kirilenko *et al.* [5].

temperatures in the observed frequency range of 8.5 and 23 MHz as shown in Table 5 and Fig. 13 in the case of the $CsHgCl_3$ sample which spent a year after preparation of the melt (hereafter Sample A). Space group $P3_2$ indicated that nine kinds of Cl atom exist as an asymmetric unit in the crystal. Therefore, nine ^{35}Cl NQR lines should be observed at room temperature and also at 77 K, or according to the Hg−Cl bond lengths of around 2.35 Å, six NQR lines may be expected in the observed frequency range, if there is no phase transition at temperatures between 77 K and room temperature. Kirilenko *et al.* reported that nine ^{35}Cl NQR lines were observed at 77 K and four NQR lines at 293 K [5], and that the phase transition occurred at 85 K, and moreover the space group was $Pm3m$ at room temperature. Our NQR results at room temperature are in agreement with the report by them, but we could not observe NQR signals around 77 K and the temperature dependence shows that there is no phase transition in the observed temperature range between 88 and 273 K. Because NQR signals always appear together with side bands of the frequency difference of which is equal to the quenching frequency of about 40 KHz, we can hardly detect the close multiplicity. Therefore, it may be possible to miss NQR signals at around 77 K. When the phase transition occurs at 85 K, the room temperature phase has to have four non-equivalent positions of Cl atoms and, therefore, the space group $P3_2$ is difficult to explain the number of NQR signals.

We tried to obtain the crystal from the hydrochloric acid solution of stoichiometric mixture of CsCl and $HgCl_2$, because the crystal from the melt may well appear accompanying with crystals of different component. The crystal formed from the solution showed four NQR signals with same frequencies as Sample A. Then we tried to determine the crystal structure by means of single crystal X-ray diffraction method but we did not succeed to analyze until now.

Different NQR results were obtained in the case of the fresh sample immediately after preparation from melt (hereafter Sample B): Three NQR lines were observed at temperatures between 80 and 350 K. These thee NQR lines of Sample B were almost the same as the lower three NQR lines of Sample A as shown in Fig. 14 and Table 6. Scaife reported almost the same ^{35}Cl NQR spectra as sample A without ν_2 at 298 K [13] as shown in Fig. 14. In addition, when the sample of Sample A and B annealed at 480 K for a half day, only one ^{35}Cl NQR line could be observed after cooling to room temperature and then several months later both Sample A and B show same NQR lines as before annealing. Albarski *et al.* showed that the crystal of space group $P3_2$ con-

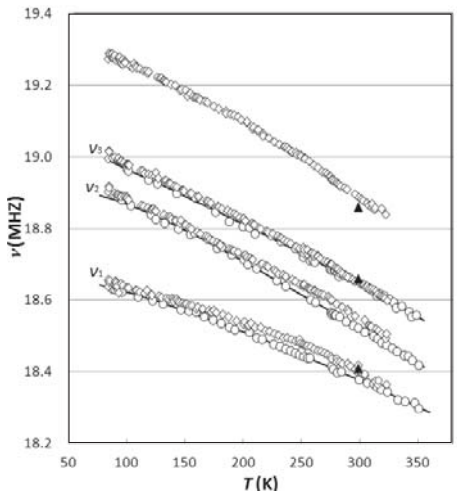

Fig. 14. Temperature dependence of ^{35}Cl NQR frequencies of $CsHgCl_3$ (Sample B). The solid line shows the fitting curve by least-squares method (Appendix I). The diamond squares show results of Sample A. The triangles show results by Scaife [13].

Table 6. The observed ^{35}Cl NQR frequencies of metastable $CsHgCl_3$.

T (K)	95	298
ν (MHz)	18. 62, 18. 88 18. 97	18. 38, 18. 52 18. 65

18.41, 18.66, and 18.86 MHz at 298 K [13]

verted into the crystal of space group $Pm3m$ under high pressure [11]. The space group $Pm3m$ forces that one ^{35}Cl NQR line should be expected as mentioned above. $CsHgCl_3$ must be polymorphic under certain conditions of temperature and /or pressure.

$CsHg_2Cl_5$

The crystal structure of $CsHg_2Cl_5$ was reported by Pakhomov *et al.* [12] and is monoclinic, space group $P2_1$ with a=8.136(13), b=6.126(2), c=9.840(12) Å, and β =100.95(13)°, Z=2. Seven of nine chlorine atoms as asymmetric unit in the crystal occupied at the sites of the occupation factor which was not equal to 1. Therefore, the chlorine positions were in disordered position. They reported also NQR frequencies observed at 293 K; 11.019, 13.844, 21.857, 22.496, and 22.897 MHz [12]. Normally the chlorine atom in the disordered state shows the broad NQR line. It is difficult to detect by our continuous wave method, however it could be detected by the pulse method, because the electric field gradient at the disordered chlorine site is not definite. On the other hand, we could observed four ^{35}Cl NQR lines and the frequencies around 293 K are considerably different from their results as listed in Table 7. No NQR line could be observed at around 77 K and three NQR lines appeared at around 100 K with increasing temperature. The temperature dependence of ^{35}Cl NQR

Table 7. The observed ^{35}Cl NQR frequencies of $CsHg_2Cl_5$.

T (K)	101	273 (286)
ν (MHz)	21. 81, 22. 47, 22. 86	20. 89, 22. 0, 722. 31, (21. 23)

11.019, 13.844, 21.857, 22.496, and 22.897 MHz at 293 K [12]. 18.64, 18.88, 18.97, 19.15, 19.23, 19.36, 20.72, 21.68, 21.87, 22.39, 22.52, and 22.87 MHz [5].

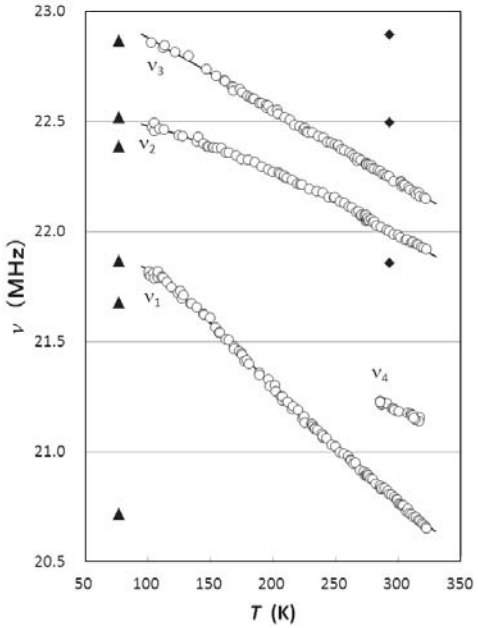

Fig. 15. Temperature dependence of ^{35}Cl NQR frequencies of $CsHg_2Cl_5$. The solid line shows the fitting curve by least-squares method (AppendixI). The diamond squares show the result by Parkhomov *et al* [12] The triangles show the result by Kirilenko *et al.* [5].

lines is shown in Fig. 15 and ν_4 NQR line appeared at around 285 K with increasing temperature. Kirilenko *et al.* reported twelve ^{35}Cl NQR lines at 77 K as is also shown in Fig. 15 [5]. Taking their result into consideration, there may be a phase transition at around 100 K. In addition, in the case of the sample of $CsHg_2Cl_5$ annealed at 480 K for a half day, ν_4 NQR line disappeared after cooling to room temperature.

$CsHg_5Cl_{11}$

Three ^{35}Cl NQR lines with intensity ratio of 3:3:1 in decreasing-frequency order were observed as listed in Table 8 and the temperature dependence of NQR frequencies are shown in Fig. 16. The intensity of the ν_3 line decreased at temperatures approaching the liquid nitrogen temperature as shown in Fig. 16. Scaife reported three ^{35}Cl NQR lines at 298 K [13] and the frequencies of three lines are the same frequencies as those of $CsHg_5Cl_{11}$ as listed in Table 8. There is no indication of a phase transition at temperatures between 85 and 322 K.

Table 8. The observed ^{35}Cl NQR frequencies of $CsHg_5Cl_{11}$.

T (K)	85 (176)	273
ν (MHz)	20.72, 21.70, (22.17)	20.40, 21.24, 21.92

20.34, 21.15, and 21.81 MHz at 298 K [13].

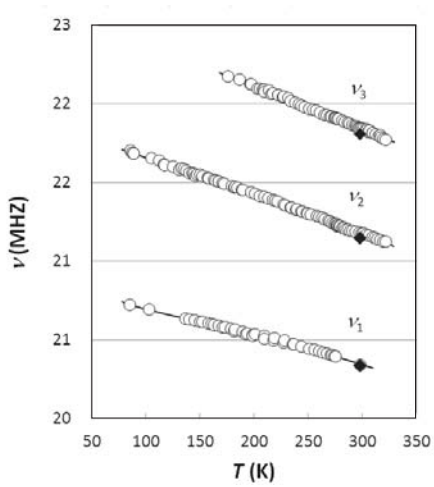

Fig. 16. Temperature dependence of ^{35}Cl NQR frequencies of $CsHg_2Cl_5$. The solid line shows the fitting curve by least-squares method (Appendix I). The diamond squares show the result by Scaife [13].

The dependence of ^{35}Cl NQR frequencies on the Hg–Cl bond distance

The ^{35}Cl NQR frequency is expressed by the next equation,

$$\nu = (e^2Qq/2h)(1+\eta^2/3)^{1/2}, \quad (1)$$

where e^2Qq/h is the quadrupole coupling constant for the observed Cl atom, eQ the qauadrupole moment of ^{35}Cl atom, eq the maximum component of electric field gradient (EFG) around the observed ^{35}Cl atom, and η the asymmetry parameter of the electric field gradient. The asymmetry parameter η for the terminal Cl atom can be assumed to be zero and the value of eq is mainly ascribed to the covalent bond character of Hg–Cl bond. Therefore, the unbalance p-electron number defined by the next equation,

$$U_p = e^2Qq/e^2Qq_{atom}, \quad (2)$$

where e^2Qq_{atom} is the atomic quadrupole coupling constant of ^{35}Cl atom, and is related to the ionic character of the Hg–Cl, i, according to Townes-Dailey theory, [14] as shown below,

$$U_p = (1-i)(1-s), \quad (3)$$

where s is the s-character of the Cl bonding orbital and is normally 0.15.

Generally speaking, as the Hg–Cl bond length increases, the iconicity i approaches to 1 and therefore ^{35}Cl NQR frequency for the terminal Cl atom can be dependent on the Hg–Cl bond length. Furthermore the maximum component of EFG of a single electron is expressed by the following equation,

$$eq(r) = -e(3\cos^2\theta - 1)/r^3, \quad (4)$$

which shows the dependence of $1/r^3$.The origin of the maximum component of EFG is mostly due to the bonding electron and therefore NQR fre-

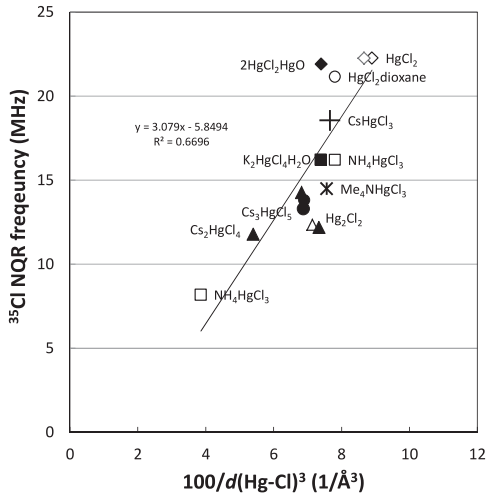

Fig. 17. The dependence of ^{35}Cl NQR frequency on Hg−Cl bond distance in $HgCl_2$ complexes [S2].

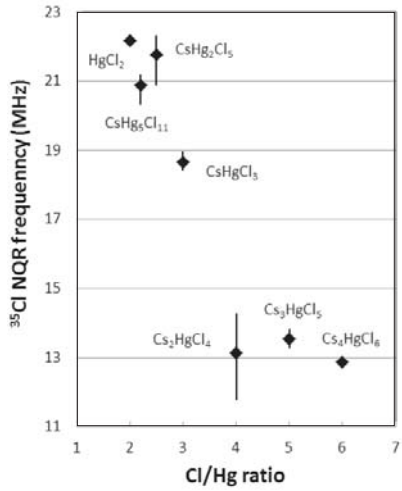

Fig. 18. The dependence of ^{35}Cl NQR frequency on ratio of Cl/Hg. Solid perpendicular bars indicate the observed frequency range.

quency can be expected to be dependent on $1/d(\mathrm{Hg-Cl})^3$, as illustrated in Fig 17. The sum of van der Waals radius of Hg (1.55 Å) and Cl (1.75 Å) or ionic radius Cl^- (1.81 Å) is 3.30~3.36 Å is comparable with 3.8 Å of the Hg−Cl distance which makes zero of the fitting equation of $\nu(^{35}\mathrm{Cl})=3.079/d(\mathrm{Hg-Cl})^3-5.8494$. In other word, there is no interaction between Hg and Cl atoms which are away from each other more than around 3.3 Å. In addition, Fig. 18 shows the dependence of ^{35}Cl NQR frequency on the ratio of the number of Cl atoms to Hg atoms. There is a large difference between the value of three ($CsHgCl_3$) and four (Cs_2HgCl_4). This fact may show the change of coordination number of Hg atom in the crystal from about two to four: $CsHgCl_3$ [10] and $CsHg_2Cl_5$ [11] have the coordination scheme like $HgCl_2$, and Cs_2HgCl_4 [8] and Cs_3HgCl_5 [6] have tetrahedral $HgCl_4^-$ ion. The increase of number of the coordinated the Cl^- ion to Hg atom makes each Hg−Cl bond more ionic and then ^{35}Cl NQR frequency decreases.

Conclusion

Hg_3OCl_4 shows one ^{35}Cl NQR line in agreement with the result of X-ray work [1]. Cs_4HgCl_6 may be metastable form and it turns into CsCl and Cs_3HgCl_5. Cs_3HgCl_5 and Cs_2HgCl_4 of room temperature phase has $HgCl_4^{2-}$ ion with *Cs* symmetry [6, 8]. The structure of $CsHgCl_3$ is not conclusive probably because of the complex polymorphism. $CsHg_2Cl_5$ is not in agreement with the report by Pakhomov *et. al.* [12], but the Cl coordination scheme around the Hg atom must be like $HgCl_2$ (Fig. 18). $CsHg_5Cl_{11}$ has also coordination scheme like $HgCl_2$.

Experimental Section

Sample preparation

Hg_3OCl_4 was prepared by leaving the $HgCl_2$−NaOH−H_2O mixture at room temperature for about ten month according to Ref. [1]. $Hg_3O_2Cl_2$ was prepared according Ref. [2].

Cs_4HgCl_6, Cs_3HgCl_5, Cs_2HgCl_4, $CsHgCl_3$, $CsHg_2Cl_5$, and $CsHg_5Cl_{11}$ are prepared by melting stoichiometric mixture of CsCl and $HgCl_2$ according to Ref. [5].

NQR measurement

^{35}Cl NQR line the frequency range of 8.5~35 MHz was searched by using Dean-type external-quenching super-regenerative oscillator made of 6 C4 tubes with Zeeman magnetic modulation. The NQR frequencies were determined by counting method. The temperature measurement was done by means of cupper-constantan thermocouple.

X-ray measurement

The X-ray powder diffraction pattern at room temperature was measured using RIGAKU RINT 1100 (Cu-Kα: $\lambda_{\alpha 1}$=1.5406 Å) and single crystal structure was determined using RIGAKU SATURN 724 and Program package CRYSTALSTRUCTURE 3.8.2 in Analytical Research Center of Saga University.

References

[1] Ar. Weiss, G. Nagorsen, and, Al. Weiss, *Z. Anorg. Allg. Chem.* **274**, 151-68 (1953).

[2] S. Scavnicar, *Acta Crystallogr.* **8**, 379-83 (1955).

[3] RIETAN 2000 for Windows is a multi-purpose pattern fitting system developed by F. Izumi.
F. Izumi and T. Ikeda, *Mater. Sci. Forum*, **321-324**, 198-203 (2000). MERCURY 3.1.1 is a crystal structure visualization, exploration and analysis system from Cambridge Crystallographic Data Centre (CCDC).

[4] H. W. Foote, *Am. Chem. J.* **30**, 339 (1903).

[5] V. V. Kirilenko, V. I. Pakhomov, A. Ya. Mikhailova, Sh. R. Lotfulin, M. V. Simonov, A. V. Medvedev, and R. N. Shchelokov, *Izv. Akad. Nauk SSSR, Neorg. Mater.* **20** (11), 1911-15 (1984).

[6] W. Clegg, M. L. Brown, and L. J. A. Wilson, *Acta Crystallogr.* **B32**, 2905-2906, (1976).

[7] A. A. Boguslavskii, D. L. Zagorskii, I. S. Zheludev, V. V. Kirilenko, R. Sh. Lotfullin, and V. I. Pakhomov, *Kristallografiya* **34**, 759-760 (1989).

[8] S. A. Linde, A. Ya. Mikhailova,V. I. Pakhomov, V. V. Kirilenko, and V. G. Shul'ga, *Koordinats. Khim.* **9** (7), 998-999 (1983).

[9] V. I. Pakhomov, A. V. Goryunov, I. N. Ivanova-Korfini, A. A. Boguslavskii, R. Sh. Lotfullin, *Z. Neorg. Khim.* **37** (3) 526-530 (1992).

[10] V. I. Parkhomov and A. V. Goryunov, *Z. Neorg. Khim.* **38** (9), 1501-8 (1993).

[11] O. Albarski, H. Hillebrecht, H. W. Rotter, and G. Thiele, *Z. Anorg. Allg. Chem.* **626** (6), 1296-1304 (2000).

[12] V. I. Pakhomov, A. V. Goryunov, I. N. Ivanova-Korfini, A. A. Boguslavskii, R. Sh. Lotfullin, *Zh. Neorg. Khim.* **36** (6), 1408-14 (1991).

[13] D. E. Scaife, *Aust. J. Chem.*, **24**, 1753-1770 (1971).

[14] C. H. Townes and B. P. Dailey, *J. Chem. Phys.* **17**, 782 -796 (1949).

[S1] *e. g.* B. Bagautdinov, A. Jobst, J. Ludecke, S. van Smaalen, *Acta Crystallographica,* **B57** (3), 231-236, (2001). B. Sh. Bagautdinov, I. D. Brown, Yu. I. Yuzyuk, V. P. Dmitriev, *Fiz. Tverd. Tela* (Sankt-Peterburg), **43** (2), 350-354, (2001). K. Suzuki, S. Ishimaru, R. Ikeda, *J. Phys. Soc. Jpn.* **69** (3), 729-733, 2000.

[S2] See Ref. [13]. References therein.

Appendix

Ⅰ. *Fitting parameters of* $\nu = a + b/T + c\times T + d\times T^2$ *and standard deviation by the least squares method*

Hg_3OCl_4	a (MHz)	b (MHz·K)	c (MHz/K)	d (MHz/K^2)	Standard Deviation (MHz)
$\nu_1(47)$ a)	22. 4625	−3. 2509	-1.5580×10^{-3}	-1.4960×10^{-6}	1.324×10^{-3}

a) The number of data in parenthesis.

Cs_3HgCl_5	a(MHz)	b(MHz·K)	c(MHz/K)	d(MHz/K^2)	Standard Deviation (MHz)
$\nu_1(41)$ a)	13. 5286	2. 0110	-3.1323×10^{-4}	-2.2233×10^{-6}	5.095×10^{-4}
$\nu_2(55)$	14. 5480	−4. 2445	-2.9830×10^{-3}	1.2704×10^{-6}	0.678×10^{-4}

a) The number of date in parenthesis.

Metastable Cs_4HgCl_6	a(MHz)	b(MHz·K)	c(MHz/K)	d(MHz/K^2)	Standard Deviation (MHz)
$\nu_1(49)$ a)	13. 3441	−1. 3715	-1.3128×10^{-3}	-1.4073×10^{-6}	7.854×10^{-3}

a) The number of data in parenthesis.

Cs_2HgCl_4	a(MHz)	b(MHz·K)	c(MHz/K)	d(MHz/K^2)	Standard Deviation (MHz)
$\nu_1(22)$ a)	12. 8658	−30. 1637	-3.4964×10^{-3}	-1.5026×10^{-6}	1.510×10^{-3}
$\nu_2(17)$	11. 1967	53. 0647	1.1446×10^{-2}	-3.7588×10^{-5}	1.898×10^{-3}
$\nu_3(24)$	11. 0049	88. 7072	2.2391×10^{-2}	-8.7590×10^{-5}	1.496×10^{-3}
$\nu_4(22)$	14. 3101	29. 0896	5.7513×10^{-3}	-2.7798×10^{-5}	1.180×10^{-3}
$\nu_5(53)$	12. 1862	−48. 2153	-1.0968×10^{-4}	-2.7784×10^{-6}	1.263×10^{-3}
$\nu_6(58)$	11. 1130	148. 4443	3.5643×10^{-3}	-6.1071×10^{-6}	1.458×10^{-3}
$\nu_7(63)$	13. 3418	159. 1794	3.7496×10^{-3}	-9.0754×10^{-6}	1.436×10^{-3}

a) The number of data in parenthesis.

$CsHgCl_3$ Sample A	a(MHz)	b(MHz·K)	c(MHz/K)	d(MHz/K^2)	Standard Deviation (MHz)
ν_1 (98) a)	18. 5858	5. 6908	2.5722×10^{-4}	-3.1065×10^{-6}	4.876×10^{-4}
$\nu_2(100)$	18. 9447	3. 8484	-7.9210×10^{-4}	-1.9041×10^{-6}	3.849×10^{-4}
$\nu_3(113)$	19. 0138	5. 3061	-6.4012×10^{-4}	-2.1139×10^{-6}	3.206×10^{-4}
$\nu_4(116)$	19. 3603	1. 3349	-8.5407×10^{-4}	-2.4518×10^{-6}	3.901×10^{-4}

a) The number of data in parenthesis.

$CsHgCl_3$ Sample B	a(MHz)	b(MHz·K)	c(MHz/K)	d(MHz/K^2)	Standard Deviation (MHz)
$\nu_1(42)$ a)	18. 7427	−1. 6915	-9.4517×10^{-4}	-8.5757×10^{-7}	5.100×10^{-4}
$\nu_2(39)$	19. 1406	−7. 4974	-1.9494×10^{-3}	-1.2382×10^{-7}	6.245×10^{-4}
$\nu_3(42)$	19. 0702	2. 0168	-1.1342×10^{-3}	-1.0257×10^{-6}	8.395×10^{-4}

a) The number of data in parenthesis.

$CsHg_2Cl_5$	a(MHz)	b(MHz·K)	c(MHz/K)	d(MHz/K^2)	Standard Deviation (MHz)
ν_1(108)[a]	23. 4048	−57. 3011	-1.1007×10^{-2}	-9.4256×10^{-6}	8.558×10^{-4}
ν_2 (75)	22. 7388	−7. 3252	1.5627×10^{-3}	-2.8966×10^{-6}	8.440×10^{-4}
ν_3 (78)	23. 2673	−3. 0166	-3.6055×10^{-3}	5.3578×10^{-8}	7.238×10^{-4}

a) The number of data in parenthesis.

$CsHg_5Cl_{11}$	a(MHz)	b(MHz·K)	c(MHz/K)	d(MHz/K^2)	Standard Deviation (MHz)
ν_1(42)[a]	20. 6329	10. 7283	-1.1174×10^{-4}	-3.2275×10^{-6}	6.850×10^{-4}
ν_2(86)	21. 8714	0. 3465	-2.0471×10^{-3}	-9.2231×10^{-7}	5.009×10^{-4}
ν_3(62)	22. 5494	6. 5638	-2.1787×10^{-3}	-8.6126×10^{-7}	6.133×10^{-4}

a) The number of data in parenthesis.

Ⅱ. *The atomic coordinates obtained from Rietveld analysis by means of Rietan2000.*

Hg_3OCl_4	Cubic, $P2_13$, a=9. 2341(2) Å, Z= 4			
Atom(Species)	x	y	z	B／Å^2
Hg(Hg^{2+})	0. 2290(2)	0. 1780(2)	0. 5170(2)	1. 89(6)
O(O)	0. 8607(35)	0. 8607(−)	0. 8607(−)	6. 05(1. 78)
Cl_1(Cl)	0. 2970(12)	0. 0086(14)	0. 3347(11)	0. 98(0. 25)
Cl_2(Cl^-)	0. 4138(16)	0. 4138(−)	0. 4138(−)	6. 36(1. 00)

Cs_3HgCl_5	Orthorhombic, *Pnma*, a=8. 9265(7), b=10. 7735(8), c=13. 5126(10) Å, Z= 4			
Atom(Species)	x	y	z	B／Å^2
Cs_1(Cs^+)	0. 0848(14)	0. 2500(−)	−0. 0505(8)	3. 0[a]
Cs_2(Cs^+)	0. 0924(10)	0. 0256(6)	0. 6679(7)	3. 0[a]
Hg(Hg^{2+})	0. 1994(4)	0. 2500(−)	0. 3850(6)	2. 0[a]
Cl_1(Cl^-)	−0. 0004(45)	0. 2500(−)	0. 4987(32)	2. 2[a]
Cl_2(Cl^-)	0. 1166(50)	0. 2500(−)	0. 1795(28)	2. 2[a]
Cl_3(Cl^-)	0. 3229(30)	0. 4543(23)	0. 4247(18)	2. 2[a]
Cl_4(Cl^-)	0. 3039(46)	0. 2500(−)	0. 7546(25)	2. 2[a]

a) Fixed value.

Cs_2HgCl_4	Orthorhombic, *Pnma*, a=9. 8916(5), b=7. 6073(4), c=13. 4217(7) Å, Z= 4			
Atom(Species)	x	y	z	B／Å^2
Cs_1(Cs^+)	0. 4827(7)	0. 2500(−)	−0. 6815(5)	3. 0[a]
Cs_2(Cs^+)	0. 1274(7)	0. 2500(−)	−0. 4018(6)	3. 0[a]
Hg(Hg^{2+})	0. 2165(5)	0. 2500(−)	−0. 0762(4)	2. 0[a]
Cl_1(Cl^-)	0. 3181(26)	0. 2500(−)	−0. 8936(18)	2. 2[a]
Cl_2(Cl^-)	0. 4739(20)	0. 2500(−)	−0. 4113(21)	2. 2[a]
Cl_3(Cl^-)	0. 3156(18)	−0. 0127(21)	−0. 1524(12)	2. 2[a]

a) Fixed value.

$CsHgCl_3$	Cubic, $Pm\,3\,m$, $a=5.4316(1)$, $Z=1$			
Atom(Species)	x	y	z	B／Å^2
Cs(Cs^+)	0.0000(−)	0.0000(−)	0.0000(−)	4.69(10)
Hg(Hg^{2+})	0.5000(−)	0.5000(−)	0.5000(−)	2.28(7)
Cl(Cl^-)	0.5000(−)	0.0000(−)	0.5000(−)	8.83(31)

$CsHgCl_3$	Trigonal, $P\,3_2$, $a=13.2976(6)$, $c=9.4177(6)$ Å, and $Z=9$			
Atom(Species)	x	y	z	B／Å^2
Cs_1(Cs^+)	0.8832(44)	0.7756(33)	0.1930(63)	1.0[a]
Cs_2(Cs^+)	0.5670(50)	0.7767(42)	0.5309(74)	1.0[a]
Cs_3(Cs^+)	0.5344(37)	0.0944(31)	−0.1630(60)	1.0[a]
Hg_1(Hg^{2+})	0.5561(31)	0.7756(33)	0.0000(−)[a]	1.0[a]
Hg_2(Hg^{2+})	0.5536(35)	0.0981(21)	0.3466(43)	1.0[a]
Hg_3(Hg^{2+})	0.8782(32)	0.0967(21)	0.6648(70)	1.0[a]
Cl_1(Cl^-)	0.365(12)	0.746(12)	−0.147(21)	1.0[a]
Cl_2(Cl^-)	0.683(12)	0.750(14)	0.156(15)	1.0[a]
Cl_3(Cl^-)	0.548(15)	0.229(10)	0.155(15)	1.0[a]
Cl_4(Cl^-)	0.559(16)	0.955(13)	0.146(20)	1.0[a]
Cl_5(Cl^-)	0.912(15)	0.256(13)	0.811(17)	1.0[a]
Cl_6(Cl^-)	0.908(11)	0.959(15)	0.524(18)	1.0[a]
Cl_7(Cl^-)	0.718(13)	0.104(12)	0.483(23)	1.0[a]
Cl_8(Cl^-)	0.739(11)	0.404(10)	−0.195(15)	1.0[a]
Cl_9(Cl^-)	0.679(11)	0.934(10)	−0.144(18)	1.0[a]

a) Fixed value